Published in final edited form as:

*Acta Biomater*. 2016 January ; 29: 42–51. doi:10.1016/j.actbio.2015.10.039.

# Mineral Particles Modulate Osteo-chondrogenic Differentiation of Embryonic Stem Cell Aggregates

**Yun Wang**[a], **Xiaohua Yu**[b], **Christopher Baker**[c], **William L. Murphy**[b], and **Todd C. McDevitt**[a,d,*]

[a] Gladstone Institute of Cardiovascular Disease, The Gladstone Institutes, San Francisco, California, 94158, USA

[b] Departments of Biomedical Engineering & Orthopedics and Rehabilitation, University of Wisconsin-Madison, Madison, Wisconsin, 53705, USA

[c] The Wallace H. Coulter Department of Biomedical Engineering, Georgia Institute of Technology and Emory University, Atlanta, Georgia, USA

[d] Department of Bioengineering and Therapeutic Sciences, University of California San Francisco, San Francisco, California, USA

## Abstract

Pluripotent stem cell aggregates offer an attractive approach to emulate embryonic morphogenesis and skeletal development. Calcium phosphate (CaP) based biomaterials have been shown to promote bone healing due to their osteoconductive and potential osteoinductive properties. In this study, we hypothesized that incorporation of CaP-coated hydroxyapatite mineral particles (MPs) within murine embryonic stem cell (ESC) aggregates could promote osteo-chondrogenic differentiation. Our results demonstrated that MP alone dose-dependently promoted the gene expression of chondrogenic and early osteogenic markers. In combination with soluble osteoinductive cues, MPs enhanced the hypertrophic and osteogenic phenotype, and mineralization of ESC aggregates. Additionally, MPs dose-dependently reduced ESC pluripotency and thereby decreased the size of teratomas derived from MP-incorporated ESC aggregates *in vivo*. Our data suggested a novel yet simple means of using mineral particles to control stem cell fate and create an osteochondral niche for skeletal tissue engineering applications.

### Keywords

Mineral microparticles; Differentiation; Osteo-chondrogenesis; Embryonic stem cells

*Correspondence information for corresponding author: Todd C. McDevitt, Ph.D., Gladstone Institutes, 1650 Owens Street, San Francisco, CA 94158, USA, Phone: +1-415-734-2875, Fax: +1-415-355-0960, todd.mcdevitt@gladstone.ucsf.edu.



**Disclosures**

The authors indicate no potential conflicts of interest.

## 1. Introduction

Pluripotent stem cells (PSCs) can differentiate into all mesodermal cell types including chondrocytes and osteoblasts, therefore representing a powerful resource for the regenerative therapy of skeletal defects and degeneration [1-5]. The successful application of PSCs primarily depends on their direct differentiation into specific lineages, which are both governed by biochemical and biophysical cues [6-8]. Osteo-chondrogenic lineage-specific differentiation of stem cells is commonly controlled by supplementing culture media with osteoinductive factors including β-glycerophosphate (β-GP), ascorbic acid, dexamethasone, and/or growth factors such as vitamin D3, transform growth factor βs (TGFβs), and bone morphogenetic proteins (BMPs) [3, 5, 9, 10]. Alternatively, the morphogenic microenvironment of stem cells can also be engineered via the intrinsic physical properties of biomaterials [11]. The surface chemistry, topography, and stiffness of biomaterials can provide dynamic multiparametric control to instruct emergent cellular behaviors and modulate chondrogenic and osteogenic differentiation [12-15].

Calcium phosphate (CaP)-based biomaterials have been widely employed as bone graft substitutes for dental and bone implants and commonly used for coating metallic implants [16-18]. Recent studies have demonstrated that osteogenic differentiation of adult stem cells, PSC-derived mesenchymal stem cells, and PSCs can be achieved by culturing stem cells with CaP-containing hydrogels, matrices, or scaffolds in the presence or even absence of osteoinductive soluble factors [4, 19-24]. Hydroxyapatite (HA) is one of the most commonly used CaP-based bone graft substitutes in orthopedic practices because of the similarity of its osteoconductivity and chemical composition to that of bone mineral [18, 25]. HA-based biomaterials have been extensively used to promote bone regeneration [4, 26]. However, it has been shown that the bioactivity of CaP-based biomaterials may be influenced by the mineral's nanostructure, crystallinity, and dissolution rate, with higher dissolution rate resulting in release of calcium and inorganic phosphate ions, leading to increased osteogenesis [25]. CaP-based microparticles with high dissolution rates have recently been developed by incubating HA microparticles in a modified simulated body fluid solution to form biomimetic CaP coatings [27, 28]. Nevertheless, it is unknown how mineral-coated particles (MPs) can modulate the differentiation of PSCs toward osteo-chondrogenic lineages.

Porous scaffolds, hydrogels, and cell carriers have been used to provide cells with a 3D microenvironment to support stem cell culture and differentiation [20-22, 29, 30]. Alternatively, a more physiologically relevant 3D microenvironment can be emulated through cell self-assembly, which has been applied to form multicellular aggregates in various cells types [31-33]. In particular, PSC aggregates are capable of recapitulating various morphogenetic processes associated with embryonic development and thus have been used to form various highly structured and functional tissues commonly referred to as "organoids" [34-38]. PSC aggregates mimic the high cell density and cell-cell interactions characteristic of mesenchymal condensation that is a critical stage that precedes both intramembranous and endochondral bone formation [39], and thus 3D aggregates represent a physiologically relevant model to examine osteo-chondrogenic differentiation of PSCs in response to exogenous cues. More importantly, incorporation of biomaterial microparticles

within cell aggregates enables direct examination of cell-biomaterial interactions that have been shown to regulate stem cell fate as a function of material properties [40-42].

Therefore, the objective of this study was to examine the use of a combinatorial biomaterial-PSC aggregate platform to study skeletal morphogenesis of PSCs in response to CaP-coated mineral particles. Different amounts of MPs were incorporated within murine embryonic stem cell (ESC) aggregates to assess their effects on osteo-chondrogenic differentiation and pluripotency *in vitro* and *in vivo*. The expression of phenotypic markers, extracellular matrix components, and mechanical properties of aggregates were examined in the absence or in combination with soluble osteoinductive factors. This study establishes a novel approach to engineer a pro-osteo-chondrogenic microenvironment of ESC aggregates via incorporation of MPs, and therefore pave a new path for regenerating skeletal tissues.

## 2. Materials and methods

### 2.1. Mineral particle preparation

Mineral particles (MPs) were prepared using a method reported previously [28]. Briefly, hydroxyapatite microparticles (Plasma Biotal LTD, UK) with an average size of between 3-5 μm in diameter were used as a starting material. HA MPs (100 mg) were incubated in 50 mL of modified simulated body fluid (mSBF) with 2X the concentration of calcium and phosphate of human blood plasma in a conical tube with constant rotation to form the mineral coating on their surfaces at 37 ºC. The mSBF was prepared by dissolving NaCl (141mM), KCl (4.0mM), $MgSO_4$ (0.5mM), $MgCl_2$ (1.0mM), $NaHCO_3$ (4.2mM), $CaCl_2$ (5.0mM), and $KH_2PO_4$ (2.0mM) in de-ionized water, and the pH was adjusted to 6.8 using 2N HCl/NaOH. The mSBF was refreshed daily during the seven day incubation period, and the MPs were collected after rinsing with deionized water and lyophilization.

### 2.2. Embryonic stem cell aggregate culture and differentiation

Murine D3 ESCs (ATCC, Manassas, VA) were cultured and expanded in ESC expansion media consisting of DMEM (Mediatech, Herndon, VA), 15% fetal bovine serum (Hyclone, Logan, UT), 100 U/mL penicillin, 100 μg/mL streptomycin, 2.5 μg/mL amphotericin, 2 mM L-glutamine, 1× non-essential amino acid solution (Mediatech), 0.1 mM 2-mercaptoethanol (Fisher Scientific, Fairlawn, NJ), and supplemented with $10^3$ U/mL of leukemia inhibitory factor (LIF, ESGRO, Chemicon, Temecula, CA) . When 2D ESC cultures were used to compare the effects of MPs on ESC pluripotency, LIF was not supplemented in the ESC expansion media during the last 24 hr of culture. ESC cultures (~70% confluent) were trypsinized into a single cell suspension to form ESC aggregates by forced aggregation in polydimethylsiloxane microwell inserts (400 μm diameter) [43]. Briefly, $6.0 \times 10^6$ cells in 3 mL of basal media (ESC expansion media without LIF) were added to each insert in a 6-well plate to form aggregates (~1000 cells each). After 16 hrs of incubation in the microwells, ESC aggregates with or without MPs were transferred to suspension culture on a rotary orbital shaker (45 rpm) in basal media (BM) for up to 14 days. In order to promote osteochodrogenic differentiation, aggregates were cultured in differentiation media (DM) from day 5 to day 14, which consisted of BM supplemented with 5 mM β-GP (Sigma) and 0.2 mM L-ascorbic acid 2-phosphate sesquimagnesium salt (vitamin C, Sigma). Media was

completely exchanged every two days after gravity-induced sedimentation of aggregates in 15 mL conical tubes.

### 2.3. MP incorporation within ESC aggregates

MPs were incorporated into ESC aggregates by mixing either $2\times10^6$ (1.7 mg) or $6\times10^6$ (5.1 mg) MPs with $6\times10^6$ single ESCs before forced aggregation in PDMS microwells to form MPs-aggregates at different seeding ratios of 1:3 or 1:1 (MPs:cells), respectively. The MP to cell ratios were chosen based upon several previously published studies with similarly sized microparticles and also preliminary studies with a wider range of ratios that yielded visual incorporation of mineral particles. To monitor the MP incorporation, particles ($10\times10^6$ /mL) were fluorescently labeled by incubation with 100 μM xylenol orange in PBS at 37 °C for 30 min. The labeled MPs were washed three times with PBS to remove residual unbound dye prior to incorporation within ESC aggregates (Supplementary Figure. 1). MP incorporation during the first 16 hrs of aggregation within microwell was monitored by an inverted fluorescent microscope (IX70, Olympus) equipped with a CCD camera (RT Color, Diagnostic, Spot Software V4.0.9). Formed aggregates were then transferred to suspension culture and unincorporated MPs were counted to calculate the MP incorporation efficiency using the formula:

$$\text{MP incorporation efficiency } (\%) = \left(1 - \frac{\text{unincroporated MP numbers}}{\text{total MP numbers}}\right) * 100\%$$

The distribution of labeled MPs in ESC aggregates was also examined at days 1 and 14 of culture. Cells in the aggregates were fluorescently labeled by incubation of aggregates with 2 μM calcein AM at 37 °C for 45 min. The stained aggregates were suspended in PBS during imaging with a Zeiss LSM 700-405 confocal microscope (Carl Zeiss, Inc., Jena, Germany).

### 2.4. Cell survival in ESC aggregates

The viability of cells comprising ESC aggregates at days 2 and 14 of culture was evaluated using LIVE/DEAD assay (Molecular Probes, Inc., Eugene, OR) as described previously [29]. Briefly, samples were incubated in PBS containing 2 μM calcein AM and 4μM ethidium homodimer-1 for 45 min at 37°C. The stained samples were washed three times in PBS and immediately imaged using a Zeiss LSM laser scanning confocal microscope (700-405, Carl Zeiss, Inc., Jena, Germany).

### 2.5. Biochemical assays

To quantify calcium and phosphate contents in ESC aggregates, samples (n=4) were harvested after 14 days of culture and lysed in 0.5 N HCl at 4°C for 24 hrs [44]. The concentration of calcium and phosphate in the supernatant was quantified using Calcium and Phosphate Colorimetric Assay Kits (BioVision Co., USA) according to manufacturer's instructions. Briefly, the absorbance of chromogenic complex formed between calcium ions and o-cresolphthalein was measured at 575 nm while that of chromogenic complex formed between phosphate ion and malachite green and ammonium molybdate was measured at 650

nm. For the measurement of sulfated glycosaminoglycan (sGAG) content, aggregates were digested in papain solution (125 μg/mL papain, 10mM cysteine) at 60°C overnight. The sGAG concentration in the lysate was then determined spectrophotometrically at 525 nm following the reaction with dimethylmethylene blue dye (Sigma–Aldrich, St. Louis, MO). The DNA content of cell lysates was determined fluorimetrically following the reaction with PicoGreen (Invitrogen Corporation) and used for normalization [29].

### 2.6. RNA isolation and real-time RT-PCR

Total RNA was extracted from ESC aggregates or 2D ESC cultures (n=4) using RNeasy Mini Kit (Qiagen, CA) and reverse-transcribed into cDNA using iScript cDNA synthesis kit (Bio-Rad, CA). Real-time PCR was performed using iQ™ SYBR® Green SuperMix (Bio-Rad) for pluripotent markers (*oct-4*, *nanog*, *rex-1*), chondrogenic markers (*sox9*, *col2a1*, *acan*, *col10a1*), osteogenic markers (*runx2*, *osx*, *col1a1*, *bsp*, *opn*, *ocn*), growth factors (*fgf1*, *fgf2*, *tgfβ1*, *tgfβ2*, *tgfβ3*, *bmp2*, *bmp4*, *bmp6*, *vegf*), and housekeeping gene (*s18*). The expression level of targeted genes was first normalized to the expression level of *s18* and then converted to the relative fold-change to the expression level of each gene in the “No MP in BM” group. Primer sequences and amplification conditions are listed in Supplemental Table 1.

### 2.7. Mechanical characterization of ESC aggregates

The bulk mechanical properties of ESC aggregates (8 aggregates per each experimental group) were assessed after 2 or 14 days of culture using a micron-scale parallel-plate compression test system (MicroSquisher, CellScale), which measures the force of cantilever beam deflection in response to user-defined displacements [42, 45] (Supplementary Figure 2A). All samples were tested in a PBS fluid-filled bath at room temperature. Cantilever beams of diameters from 76.2 μm to 152.4 μm were employed, depending on the stiffness and sensitivity required to measure different aggregates. Samples were compressed at a strain rate of 2.5 μ/s, and released at a rate of 2.5 μ/s in order to record any hysteresis. The Young's modulus of the aggregates was then calculated based upon a linear viscoelastic model of creep displacement behavior, as previously described [42, 45] (Supplementary Figure 2B).

### 2.8. Teratoma assay

ESC aggregates were injected subcutaneously into NOD SCID mouse to assess the effect of MPs on pluripotency of ESC aggregates *in vivo* [46]. All animal experiments were approved by the Georgia Institute of Technology Institutional Animal Care and Use Committee animal protocol. ESC aggregates (~4000 aggregates per implantation, ~1000 cells/aggregate) were collected from microwells after 24 hours of formation, resuspended in 0.2 mL PBS, and injected into dorsal subcutaneous pockets of 8 week-old male NOD SCID mice (Charles River Laboratories International Inc., MA) using a 26-gauge needle. An equal number of ESCs in a single-cell suspension (Single ESCs) harvested directly from 2D culture (~$4\times10^6$ cells) without supplementation of LIF during the last 24 hr of culture were also injected subcutaneously. One mouse received 3 injections per experimental group; thus, 4 animals in total were used in this study. Teratomas were recovered 28 days post injection by careful dissection from the surrounding host tissue and subjected to macroscopic assessments (size,

appearance) and the sizes of teratomas were measured by quantification of the cross-section area of macroscopic images of teratomas using Image J software (NIH, Bethesda, MD, USA). The teratomas were then processed for histological examination.

### 2.9. Histological Examination

ESC aggregates were fixed in 10% formalin, entrapped in Histogel (Thermo Scientific, Rockford, IL), processed and embedded in paraffin [47]. Paraffin blocks were sectioned at a thickness of 5 μm and stained with hematoxylin and eosin, safranin O and fast green, alizarin red, or von Kossa and fast red. Similarly, formalin-fixed teratomas were processed, embedded in paraffin, and 5 μm sections were taken every 100-200 μm per block (total of 50-70 sections per each teratoma) and stained with hematoxylin and eosin or safranin O and fast green. Stained sections were imaged using a Nikon Eclipse 80i equipped with a SpotFlex digital camera (Diagnostic Instruments, Sterling Heights, MI). Histomorphometric analysis of cartilage tissue within teratoma sections based on safranin O staining was performed using Image J software (NIH, Bethesda, MD, USA) in order to calculate the cartilage appearance frequency as well as the percentage of cartilage cross-sectional area in teratoma sections. Of note, one of the teratoma tissues derived from a single injection of 1:1 MP aggregates was separated into 3 small individual pieces, which were grouped together during the size measurement and the histomorphometric analysis of teratoma.

### 2.10. Statistical analysis

The data were expressed as mean ± standard error and subjected to one-way or two-way ANOVA followed by either Bonferroni post-hoc test or Kruskal-Wallis test for parametric or non-parametric data, respectively. All statistical analyses were performed using GraphPad 5.0 (GraphPad Software, Inc., La Jolla, CA). $P<0.05$ were considered to be statistically significant.

The differences in the gene expression of growth factors among ESC aggregates (with or without MPs incorporation) cultured in either basal or differentiation media 2D were further analyzed using hierarchical clustering (HCL) based on Euclidian distance and average linking clustering. A heat map presentation of HCL was generated using GENESIS software package (Graz University of Technology, Graz, Austria).

Principal component analysis (PCA) was performed to determine the effects of MP incorporation under different culture conditions on osteo-chondrogenic differentiation of ESC aggregates as described previously [48]. All data were mean-centered and scaled to unit variance. Observations (experimental groups) and phenotype variables (expression of osteo-chodrogenic markers and production of ECM contents) were organized into the rows and columns of the data matrix, respectively. The data matrix was then projected on 2 principle components (PCs) using SIMCA P+ (Umetrics, Malmö, Sweden). A 2D biplot was generated to visualize the contribution of phenotypic variables to the separation of treatment groups.

# 3. Results

## 3.1. MP incorporation within ESC aggregates

ESC aggregates with or without MPs formed similarly in the microwells within the first 16 hrs of culture (Supplementary Figure 3). MP incorporation within aggregates was proportional to the initial seeding density with 95.3±8.6% and 96.1±6.4% MP incorporation at the seeding ratios of 1:3 and 1:1 MPs:cells, respectively. (Figure 1A). MPs persisted within ESC aggregates for up to 14 days regardless of culture media (Figure 1A). MP incorporation did not appear to adversely affect ESCs viability. The majority of cells in all D2 cultures appeared viable and only a few aggregates in D14 cultures contained a small number of dead cells, but cell viability appeared to be independent of MP incorporation (Figure 1B).

## 3.2. Chondrogenic effects of MPs on ESC aggregate

In basal media (BM), MP incorporation significantly increased the expression of all the chondrogenic genes in comparison to ESC aggregates that lacked MPs (Figure 2A). However, 1:1 MP-incorporated aggregates cultured in differentiation media (DM) promoted hypertrophic differentiation as evidenced by a reduction of *sox9*, *col2a1*, and *acan* expression but increase in *col10a1* expression (Figure 2A). A small increase (10-30%) in sulfated glycosaminoglycan (sGAG) content was also observed in MP-incorporated aggregates (Figure 2B). Morphological analysis based on histological staining revealed considerable changes in the deposition pattern of sGAG due to MP incorporation and culture media. The majority of ESC aggregates lacking MPs in BM displayed relatively homogenous positive safaranin O staining (red), whereas most aggregates containing MPs exhibited a heterogeneous staining pattern, with regions of negative safranin o staining (green), especially in DM culture (Figure 2C).

## 3.3. Osteogenic effects of MPs on ESC aggregates

Compared to aggregates lacking MPs in basal media, MP aggregates expressed significantly higher levels of early osteogenic genes including *runx2*, *osx*, *col1a1* and *opn* (Figure 2A), but similar levels of more mature osteogenic markers, such as *bsp* and *ocn* (Figure 3A). MP incorporation alone did not increase calcium and phosphate deposition (Figure 3B), which was confirmed by negative staining for alizarin red and von Kossa, except for the residual MPs within aggregates (Figure 3C, Supplementary Figure 4A). The expression of all of the osteogenic markers was further increased when aggregates were cultured in differentiation media, especially in MP aggregates (Figure 3A). Simultaneously, mineralization of ESC aggregates was also enhanced in differentiation media with the highest phosphate and calcium contents was observed in 1:1 MP aggregates ($p<0.05$) (Figure 3B). Accordingly, aggregates in DM culture exhibited stronger staining for both alizarin red and von Kossa than those in BM culture. The numbers of positively stained aggregates as well as the sizes of stained regions per aggregate increased in a MP dose-dependent manner (Figure 3C). Staining of adjacent histological sections demonstrated that the regions containing calcium and phosphate deposits overlapped with the areas lacking sGAG (Supplementary Figure 4B). Altogether, these results indicated that differentiation media promoted the transition of

MP aggregates from an early osteo-chondrogenic phenotype to hypertrophic and more mature osteogenic phenotypes.

### 3.4. Effect of MPs on gene expression of growth factors by ESC aggregates

In addition to the phenotypic changes in ESC aggregates, MP incorporation also affected the gene expression of a wide range of growth factors that are important regulators of osteo-chondrogenic differentiation. In general, the gene expression of growth factors was significantly greater in aggregates with MPs than those without, and these differences were more pronounced when aggregates were cultured in differentiation media compared to basal media (Figure 4A). Hierarchical clustering further illustrated the distinct differences in expression profile of growth factors among the different groups (Figure 4B). In BM, a moderately increased expression of pro-chondrogenic factor *tgfβ3* was observed in 1:3 MP aggregates while the expression of both pro-chondrogenic factor *tgfβ1* and pro-osteogenic factors *bmp2, 4* were increased in 1:1 MP aggregates. DM cultures exhibited similar expression pattern with highly elevated expression of pro-chondrogenic genes (*tgfβ3*, *bmp6*) in 1:3 MP aggregates but prominent pro-osteogenic genes such as *bmp2* and *bmp4* in 1:1 MP aggregates (Figure 4B) .

### 3.5. Bulk mechanical stiffness of ESC aggregates

The bulk stiffness of ESC aggregates was examined to determine if the observed phenotypic changes impacted the overall mechanical properties of ESC aggregates. A significant increase in the Young's modulus of aggregates (Figure 5) was observed during the course of differentiation. ESC aggregates cultured in DM were consistently stiffer than each of their counterparts cultured in BM (Figure 5, P=0.001, 0.021, 0.014 for No MP, 1:3 MP, and 1:1 MP, respectively). However, MP incorporation did not change the average modulus values of aggregates, indicating that the increased bulk stiffness as a result of differentiation was unlikely due to the direct influence of MPs on the mechanical properties of ESC aggregates.

### 3.6. Effect of MPs on the pluripotency of ESC aggregates

Since MPs alone strongly affected the osteochondral differentiation of ESC aggregates *in vitro*, the direct influence of MPs on the pluripotency of ESCs aggregates was further examined by assessing the acute gene expression of pluripotent markers by D1 ESC aggregates. As expected, the expression of *oct-4*, *nanog*, and *rex-1* was significantly decreased by aggregate formation in the absence of LIF compared to ESCs in 2D culture (Figure 6A). Moreover, ESC aggregation with MPs led to an additional 15-25% reduction in the expression of pluripotency genes compared to aggregates lacking MPs (Figure 6A), indicating that MP incorporation accelerated the loss of pluripotency by ESC aggregates.

We further examined whether the decreased expression of pluripotency genes could subsequently affect the ability of ESC aggregates to form teratomas in NOD SCID mouse. Subcutaneous injections of either single ESCs or day 1 ESC aggregates led to the formation of teratomas with noticeable differences in size and appearance (Figure 6B). The retrieved teratomas derived from 1:1 MP aggregates appeared less vascularized and more translucent in contrast to teratomas derived from the other groups (Figure 6B). More interestingly, teratomas derived from no MP, 1:3 MP, and 1:1 MP aggregates had a significant reduction

(53.7%, 59.7% and 70.0%, respectively, P=0.0023) in size based on the quantification of cross-sectional area compared to that of teratomas derived from single ESCs, consistent with pluripotent gene expression results (Figure 6B). Microscopically, all of the teratomas were composed of multiple types of tissues containing cells characteristic of the three germ layers (Supplementary Figure 5), including ectoderm (retina-like structure, neural rosette, and epidermis), mesoderm (cartilage, bone, and muscle), and endoderm (pancreas, thyroid, and gut-like epithelium). Histomorphometric analysis of teratoma sections indicated that larger cartilaginous tissues were more prevalent in teratomas derived from 1:1 MP aggregates, although the observed differences were not statistically significant (Figure 6C).

## 4. Discussion

Harnessing the 3D differentiation and morphogenesis in PSCs aggregates represents an intriguing avenue for the understanding of embryonic development and the regenerative application of PSCs [49]. Several proof-of-concept studies have demonstrated the possibility of using biomaterial-based microparticles to modulate the 3D microenvironment of stem cell aggregates [40, 41]. However, successful induction of PSC aggregate differentiation toward specific lineages through this strategy has yet to be reported. CaP-based biomaterials are widely used in clinical therapies to promote bone formation due to their excellent biocompatibility, osteoconductivity, and putative osteoinductive potential [16-18, 25]. This study thus attempted to engineer a 3D microenvironment favorable for osteo-chondrogenic differentiation via incorporation of CaP-enriched mineral particles (MPs) within ESC aggregates.

Our results demonstrate that differential control of 3D ESC osteo-chondrogenic morphogenesis can be achieved via incorporation of MPs and soluble treatment of osteoinductive factors. As illustrated by PCA analysis (Figure 7A), the variance in cell phenotype was separated along two principal components on the PCA biplot based on their chondrogenic phenotype (*sox9*, *col2a1*, *acan*, *col10a1* expression and sGAG content) or osteogenic phenotype (*runx2*, *osx*, *col1a1*, *bsp*, *opn*, *ocn* expression as well as calcium and phosphate contents), respectively. PC1 and PC2 together captured 86% of the data variance present in all groups and separated the ESC aggregates into two trajectories, which led towards chondrogenic and osteogenic specifications (Figure 7A). Incorporation of MPs at low ratio (1:3 MP aggregates) alone resulted in a pronounced chondrogenic phenotype based on the highest expression of chondrogenic markers. Additional supplementation of soluble factors yielded an enhanced osteogenic phenotype in MP aggregates, with the highest expression of osteogenic markers and mineral deposition observed in 1:1 MP aggregates in DM culture. Furthermore, MP-free aggregates in differentiation media exhibited similar phenotypes as 1:1 MP aggregates in basal media, which suggested that chemical-induced differentiation could be mimicked by incorporating a high proportion of MPs (Figure 7A).

$Ca^{2+}$ and $PO4^{3-}$released from CaP-based biomaterials have been shown to dose-dependently modulate osteo-chondrogenic differentiation, in which higher dose of CaP promotes osteogenic differentiation but inhibits chondrogenic differentiation [25, 50]. In this study, the $Ca^{2+}$ and/or $PO^{3-}$ can be released from either incorporated MPs or βGP in the differentiation media to generate an extracellular CaP pool, of which the extracellular CaP

levels vary depending on the dose of incorporated-MPs, the type of culture media, and combinations thereof. The resulting CaP concentrations might thereby differentially favor either chondrogenic or osteogenic phenotype of ESC aggregates (Figure 7B). The relatively lower CaP level in 1:3 MP aggregates cultured in basal media promoted chondrogenic differentiation, while the differentiation propensity favored osteogenic lineages when MP aggregates were exposed to relatively higher levels of CaP upon supplementation of soluble factors in differentiation media.

Although the precise molecular mechanism of osteo-chondrogenic inductivity of CaP-based biomaterials remains unclear, it has recently been suggested that $Ca^{2+}$ and $PO^{3-}$ may activate different down-stream signaling pathways to exert their bioactivities [25, 51, 52]. A higher expression of G-protein coupled receptor 5A and regulator of G-protein signaling 2, which are involved in the enhancement of osteogenic differentiation and bone formation, have been observed when hMSCs were cultured on β-tricalcium phosphate ceramics [25]. A recent work has discovered a phosphate-mediated adenosine signaling mechanism responsible for the up-regulation of osteogenic markers (ocn, opn) when culturing hMSCs on mineralized matrices [52]. Future validation studies of calcium- and phosphate-based signaling pathways in the MP-incorporated ESC aggregate model could elucidate their roles in embryonic skeletal development as well as highlight the application of mineral particles to modulate the microenvironment for pluripotent stem cell-based skeletal regeneration.

Consistent with previous studies showing that cells exposed to soluble $Ca^{2+}$ and $PO^{4-}$or interaction with CaP-based biomaterials expressed more *bmp2*, *tgfβ1* and other growth factors [23, 25, 53, 54], MP aggregates also exhibited greater expression of pro-chondrogenic or pro-osteogenic growth factors. Additionally, the differences in the expression pattern of growth factors in response to MP doses and culture conditions according to their differentiated phenotypes could indirectly reflect the observed cell specification toward either chondrogenic or osteogenic cell fates. Furthermore, MPs have strong affinity to a wide range of GFs [27], and thereby could sequester growth factors secreted by ESCs to create a locally enriched growth factor microenvironment within aggregates to enhance cell differentiation. A recent study specifically demonstrated highly efficient sequestering of cell-secreted BMP-2 when hMSCs were cultured in contact with CaP mineral coatings similar to those used in our current study, supporting the concept of cell-secreted GF sequestering by the mineral coating [55].

Alternatively, the mechanical properties of biomaterials can modulate stem cell fate independent of their chemical properties [40, 52]. Harnessing stem cells for skeletal regeneration can be achieved by modulating the stiffness of biomaterials. The stiffness of 2D matrices has been shown to differentially regulate stem cell specification toward either smooth muscle cells or chondrogenic cells [56]. Sun *et al.* have also reported that the high mechanical strength of 3D scaffolds can promote stem cell mediated bone regeneration through endochondral ossification [57]. Unlike our previous observation that introduction of gelatin microparticles significantly increased the stiffness of human mesenchymal stem cell aggregates [42], the presence of MPs did not affect the mechanical properties of ESC aggregates. Of note, the compression test used in this study only allowed us to measure the bulk mechanical properties of entire aggregate. Therefore, we cannot rule out the possibility

that individual cells in direct contact with MPs might sense the stiffness of the MPs, which might impact osteo-chondrogenic differentiation.

A recent study by Kang *et al*. reported a significant reduction of *nanog* expression by human ESCs cultured on mineralized matrices in the absence of any osteoinductive supplements and the formation of ectopic bone without sign of teratoma when implanted *in vivo* [23]. Similarly, MP incorporation alone significantly reduced the expression of pluripotent markers by ESC aggregates in a dose-dependent manner. While implanted MP aggregates still formed teratomas *in vivo*, the discrepancy in species, injected cell numbers (4 times more ESC per injection) and significantly less amount of CaP materials used in our study could contribute to the observed differences. It is important to note that the period of *in vitro* culture was restricted to just 24 hours before *in vivo* injection of ESC aggregates, which may explain why limited formation of terminal osteochondral tissues was achieved *in vivo*. However, a higher frequency of cartilage tissue in 1:1 MP aggregates-derived teratomas was observed, suggesting that MPs might be able to promote osteo-chondrogenic differentiation of ESCs *in vivo* as well.

## 5. Conclusion

Engineering microenvironmental properties to regulate stem cell fate via biomaterials is an emerging strategy for regenerative medicine. Our proof-of-concept study successfully employed a 3D ESC aggregate model to investigate the potential of using calcium phosphate-based mineral particles to direct the differentiation of ESCs towards osteo-chondrogenic lineages as well as attenuate ESC pluripotency, although the optimal doses of mineral particles and treatment combinations suitable for either osteogenesis or chondrogenesis will need to be determined in future experiments before preceding to any preclinical studies or clinical applications. The results also indicate that bio-inductive materials and soluble cues can act in a combinatorial fashion to modulate skeletal morphogenesis of ESC aggregates. This biomaterial-ESC aggregate system can serve as a novel platform to assess the ability of biomaterials to directly specify stem cell fate and create functional skeletal tissues for regenerative therapies.

## Supplementary Material

Refer to Web version on PubMed Central for supplementary material.

## Acknowledgements

The authors would like to thank Dr. Melissa Kinney for analyzing the mechanical test data, as well as Dr. Tracy Hookway and Dr. Douglas White for helpful discussions. This research was supported by the National Institutes of Health (R01GM088291 and R01AR059916).

## References

[1]. Kuske B, Savkovic V, zur Nieden NI. Improved media compositions for the differentiation of embryonic stem cells into osteoblasts and chondrocytes. Methods in molecular biology. 2011; 690:195–215. [PubMed: 21042995]

[2]. Kawaguchi J. Generation of osteoblasts and chondrocytes from embryonic stem cells. Methods in molecular biology. 2006; 330:135–48. [PubMed: 16846022]

[3]. Oldershaw RA, Baxter MA, Lowe ET, Bates N, Grady LM, Soncin F, et al. Directed differentiation of human embryonic stem cells toward chondrocytes. Nature biotechnology. 2010; 28:1187–94.

[4]. Levi B, Hyun JS, Montoro DT, Lo DD, Chan CK, Hu S, et al. In vivo directed differentiation of pluripotent stem cells for skeletal regeneration. Proceedings of the National Academy of Sciences of the United States of America. 2012; 109:20379–84. [PubMed: 23169671]

[5]. Handschel J, Berr K, Depprich RA, Kubler NR, Naujoks C, Wiesmann HP, et al. Induction of osteogenic markers in differentially treated cultures of embryonic stem cells. Head & face medicine. 2008; 4:10. [PubMed: 18544155]

[6]. Tan S, Barker N. Engineering the niche for stem cells. Growth factors. 2013; 31:175–84. [PubMed: 24274105]

[7]. Titushkin I, Cho M. Modulation of cellular mechanics during osteogenic differentiation of human mesenchymal stem cells. Biophysical journal. 2007; 93:3693–702. [PubMed: 17675345]

[8]. Keung AJ, Kumar S, Schaffer DV. Presentation counts: microenvironmental regulation of stem cells by biophysical and material cues. Annual review of cell and developmental biology. 2010; 26:533–56.

[9]. Hu J, Smith LA, Feng K, Liu X, Sun H, Ma PX. Response of human embryonic stem cell-derived mesenchymal stem cells to osteogenic factors and architectures of materials during in vitro osteogenesis. Tissue engineering Part A. 2010; 16:3507–14. [PubMed: 20594153]

[10]. Kawaguchi J, Mee PJ, Smith AG. Osteogenic and chondrogenic differentiation of embryonic stem cells in response to specific growth factors. Bone. 2005; 36:758–69. [PubMed: 15794925]

[11]. Murphy WL, McDevitt TC, Engler AJ. Materials as stem cell regulators. Nature materials. 2014; 13:547–57. [PubMed: 24845994]

[12]. Na K, Kim SW, Sun BK, Woo DG, Yang HN, Chung HM, et al. Osteogenic differentiation of rabbit mesenchymal stem cells in thermo-reversible hydrogel constructs containing hydroxyapatite and bone morphogenic protein-2 (BMP-2). Biomaterials. 2007; 28:2631–7. [PubMed: 17331575]

[13]. Olivares-Navarrete R, Hyzy SL, Hutton DL, Erdman CP, Wieland M, Boyan BD, et al. Direct and indirect effects of microstructured titanium substrates on the induction of mesenchymal stem cell differentiation towards the osteoblast lineage. Biomaterials. 2010; 31:2728–35. [PubMed: 20053436]

[14]. Park JS, Chu JS, Tsou AD, Diop R, Tang ZY, Wang AJ, et al. The effect of matrix stiffness on the differentiation of mesenchymal stem cells in response to TGF-beta. Biomaterials. 2011; 32:3921–30. [PubMed: 21397942]

[15]. Barradas AMC, Monticone V, Hulsman M, Danoux C, Fernandes H, Birgani ZT, et al. Molecular mechanisms of biomaterial-driven osteogenic differentiation in human mesenchymal stromal cells. Integr Biol-Uk. 2013; 5:920–31.

[16]. Xie C, Lu H, Li W, Chen FM, Zhao YM. The use of calcium phosphate-based biomaterials in implant dentistry. J Mater Sci-Mater M. 2012; 23:853–62. [PubMed: 22201031]

[17]. Huang Z-M, Qi Y-Y, Du S-H, Feng G, Unuma H, Yan W-Q. Promotion of osteogenic differentiation of stem cells and increase of bone-bonding ability in vivo using urease-treated titanium coated with calcium phosphate and gelatin. Science and Technology of Advanced Materials. 2013; 14:055001.

[18]. Saikia KC, Bhattacharya TD, Bhuyan SK, Talukdar DJ, Saikia SP, Jitesh P. Calcium phosphate ceramics as bone graft substitutes in filling bone tumor defects. Indian J Orthop. 2008; 42:169–72. [PubMed: 19826522]

[19]. Shih YRV, Hwang Y, Phadke A, Kang H, Hwang NS, Caro EJ, et al. Calcium phosphate-bearing matrices induce osteogenic differentiation of stem cells through adenosine signaling. Proceedings of the National Academy of Sciences of the United States of America. 2014; 111:990–5. [PubMed: 24395775]

[20]. Marino G, Rosso F, Cafiero G, Tortora C, Moraci M, Barbarisi M, et al. beta-Tricalcium phosphate 3D scaffold promote alone osteogenic differentiation of human adipose stem cells: in vitro study. J Mater Sci-Mater M. 2010; 21:353–63. [PubMed: 19655233]

[21]. Tang M, Chen W, Weir MD, Thein-Han W, Xu HHK. Human embryonic stem cell encapsulation in alginate microbeads in macroporous calcium phosphate cement for bone tissue engineering. Acta Biomater. 2012; 8:3436–45. [PubMed: 22633970]

[22]. Tang MH, Chen WC, Liu J, Weir MD, Cheng LZ, Xu HHK. Human induced pluripotent stem cell-derived mesenchymal stem cell seeding on calcium phosphate scaffold for bone regeneration. Tissue Eng Pt A. 2014; 20:1295–305.

[23]. Kang H, Wen C, Hwang Y, Shih Y-RV, Kar M, Seo SW, et al. Biomineralized matrix-assisted osteogenic differentiation of human embryonic stem cells. Journal of Materials Chemistry B. 2014; 2:5676–88.

[24]. TheinHan W, Weir MD, Simon CG, Xu HH. Non-rigid calcium phosphate cement containing hydrogel microbeads and absorbable fibres seeded with umbilical cord stem cells for bone engineering. Journal of tissue engineering and regenerative medicine. 2013; 7:777–87. [PubMed: 22451091]

[25]. Barradas AM, Monticone V, Hulsman M, Danoux C, Fernandes H, Tahmasebi Birgani Z, et al. Molecular mechanisms of biomaterial-driven osteogenic differentiation in human mesenchymal stromal cells. Integrative biology : quantitative biosciences from nano to macro. 2013; 5:920–31. [PubMed: 23752904]

[26]. Kim S, Kim SS, Lee SH, Eun Ahn S, Gwak SJ, Song JH, et al. In vivo bone formation from human embryonic stem cell-derived osteogenic cells in poly(d,l-lactic-co-glycolic acid)/hydroxyapatite composite scaffolds. Biomaterials. 2008; 29:1043–53. [PubMed: 18023477]

[27]. Suarez-Gonzalez D, Barnhart K, Migneco F, Flanagan C, Hollister SJ, Murphy WL. Controllable mineral coatings on PCL scaffolds as carriers for growth factor release. Biomaterials. 2012; 33:713–21. [PubMed: 22014948]

[28]. Yu X, Khalil A, Dang PN, Alsberg E, Murphy WL. Multilayered Inorganic Microparticles for Tunable Dual Growth Factor Delivery. Advanced functional materials. 2014; 24:3082–93. [PubMed: 25342948]

[29]. Wang Y, Bella E, Lee CS, Migliaresi C, Pelcastre L, Schwartz Z, et al. The synergistic effects of 3-D porous silk fibroin matrix scaffold properties and hydrodynamic environment in cartilage tissue regeneration. Biomaterials. 2010; 31:4672–81. [PubMed: 20303584]

[30]. Lee YS, Lim KS, Oh JE, Yoon AR, Joo WS, Kim HS, et al. Development of porous PLGA/PEI1.8k biodegradable microspheres for the delivery of mesenchymal stem cells (MSCs). Journal of controlled release : official journal of the Controlled Release Society. 2015; 205:128–33. [PubMed: 25575866]

[31]. Burdett E, Kasper FK, Mikos AG, Ludwig JA. Engineering tumors: a tissue engineering perspective in cancer biology. Tissue engineering Part B, Reviews. 2010; 16:351–9. [PubMed: 20092396]

[32]. Bratt-Leal AM, Carpenedo RL, McDevitt TC. Engineering the embryoid body microenvironment to direct embryonic stem cell differentiation. Biotechnology progress. 2009; 25:43–51. [PubMed: 19198003]

[33]. Rettinger CL, Fourcaudot AB, Hong SJ, Mustoe TA, Hale RG, Leung KP. In vitro characterization of scaffold-free three-dimensional mesenchymal stem cell aggregates. Cell and tissue research. 2014; 358:395–405. [PubMed: 25012521]

[34]. Suga H, Kadoshima T, Minaguchi M, Ohgushi M, Soen M, Nakano T, et al. Self-formation of functional adenohypophysis in three-dimensional culture. Nature. 2011; 480:57–62. [PubMed: 22080957]

[35]. Nakano T, Ando S, Takata N, Kawada M, Muguruma K, Sekiguchi K, et al. Self-formation of optic cups and storable stratified neural retina from human ESCs. Cell stem cell. 2012; 10:771–85. [PubMed: 22704518]

[36]. Antonica F, Kasprzyk DF, Opitz R, Iacovino M, Liao XH, Dumitrescu AM, et al. Generation of functional thyroid from embryonic stem cells. Nature. 2012; 491:66–71. [PubMed: 23051751]

[37]. Spence JR, Mayhew CN, Rankin SA, Kuhar MF, Vallance JE, Tolle K, et al. Directed differentiation of human pluripotent stem cells into intestinal tissue in vitro. Nature. 2011; 470:105–9. [PubMed: 21151107]

[38]. Lancaster MA, Knoblich JA. Organogenesis in a dish: modeling development and disease using organoid technologies. Science. 2014; 345:1247125. [PubMed: 25035496]

[39]. Edwards GO, Coakley WT, Ralphs JR, Archer CW. Modelling condensation and the initiation of chondrogenesis in chick wing bud mesenchymal cells levitated in an ultrasound trap. European cells & materials. 2010; 19:1–12. [PubMed: 20077400]

[40]. Bratt-Leal AM, Carpenedo RL, Ungrin MD, Zandstra PW, McDevitt TC. Incorporation of biomaterials in multicellular aggregates modulates pluripotent stem cell differentiation. Biomaterials. 2011; 32:48–56. [PubMed: 20864164]

[41]. Bernard AB, Chapman RZ, Anseth KS. Controlled local presentation of matrix proteins in microparticle-laden cell aggregates. Biotechnology and bioengineering. 2013

[42]. Baraniak PR, Cooke MT, Saeed R, Kinney MA, Fridley KM, McDevitt TC. Stiffening of human mesenchymal stem cell spheroid microenvironments induced by incorporation of gelatin microparticles. Journal of the mechanical behavior of biomedical materials. 2012; 11:63–71. [PubMed: 22658155]

[43]. Bratt-Leal AM, Nguyen AH, Hammersmith KA, Singh A, McDevitt TC. A microparticle approach to morphogen delivery within pluripotent stem cell aggregates. Biomaterials. 2013; 34:7227–35. [PubMed: 23827184]

[44]. Hess K, Ushmorov A, Fiedler J, Brenner RE, Wirth T. TNFalpha promotes osteogenic differentiation of human mesenchymal stem cells by triggering the NF-kappaB signaling pathway. Bone. 2009; 45:367–76. [PubMed: 19414075]

[45]. Kinney MA, Saeed R, McDevitt TC. Mesenchymal morphogenesis of embryonic stem cells dynamically modulates the biophysical microtissue niche. Scientific reports. 2014; 4:4290. [PubMed: 24598818]

[46]. Hentze H, Soong PL, Wang ST, Phillips BW, Putti TC, Dunn NR. Teratoma formation by human embryonic stem cells: Evaluation of essential parameters for future safety studies. Stem Cell Res. 2009; 2:198–210. [PubMed: 19393593]

[47]. Wilson JL, Najia MA, Saeed R, McDevitt TC. Alginate encapsulation parameters influence the differentiation of microencapsulated embryonic stem cell aggregates. Biotechnology and bioengineering. 2013

[48]. Kou PM, Schwartz Z, Boyan BD, Babensee JE. Dendritic cell responses to surface properties of clinical titanium surfaces. Acta Biomater. 2011; 7:1354–63. [PubMed: 20977948]

[49]. Kinney MA, Hookway TA, Wang Y, McDevitt TC. Engineering three-dimensional stem cell morphogenesis for the development of tissue models and scalable regenerative therapeutics. Annals of biomedical engineering. 2014; 42:352–67. [PubMed: 24297495]

[50]. Gigout A, Jolicoeur M, Buschmann MD. Low calcium levels in serum-free media maintain chondrocyte phenotype in monolayer culture and reduce chondrocyte aggregation in suspension culture. Osteoarthritis and cartilage / OARS, Osteoarthritis Research Society. 2005; 13:1012–24.

[51]. Chai YC, Roberts SJ, Desmet E, Kerckhofs G, van Gastel N, Geris L, et al. Mechanisms of ectopic bone formation by human osteoprogenitor cells on CaP biomaterial carriers. Biomaterials. 2012; 33:3127–42. [PubMed: 22269651]

[52]. Shih YR, Hwang Y, Phadke A, Kang H, Hwang NS, Caro EJ, et al. Calcium phosphate-bearing matrices induce osteogenic differentiation of stem cells through adenosine signaling. Proceedings of the National Academy of Sciences of the United States of America. 2014; 111:990–5. [PubMed: 24395775]

[53]. Tada H, Nemoto E, Foster BL, Somerman MJ, Shimauchi H. Phosphate increases bone morphogenetic protein-2 expression through cAMP-dependent protein kinase and ERK1/2 pathways in human dental pulp cells. Bone. 2011; 48:1409–16. [PubMed: 21419244]

[54]. Joiakim AP, Chopra DP. Retinoic acid and calcium regulation of p53, transforming growth factor-beta 1, and transforming growth factor-alpha gene expression and growth in adenovirus 12-SV40-transformed human tracheal gland epithelial cells. American journal of respiratory cell and molecular biology. 1993; 8:408–16. [PubMed: 8476634]

[55]. Yu X, Murphy WL. 3-D Scaffold Platform for Optimized Non-viral Transfection of Multipotent Stem Cells. Journal of materials chemistry B, Materials for biology and medicine. 2014; 2:8186–93.

[56]. Burke D, Dishowitz M, Sweetwyne M, Miedel E, Hankenson KD, Kelly DJ. The role of oxygen as a regulator of stem cell fate during fracture repair in TSP2-null mice. Journal of orthopaedic research : official publication of the Orthopaedic Research Society. 2013; 31:1585–96. [PubMed: 23775935]

[57]. Sun H, Zhu F, Hu Q, Krebsbach PH. Controlling stem cell-mediated bone regeneration through tailored mechanical properties of collagen scaffolds. Biomaterials. 2014; 35:1176–84. [PubMed: 24211076]

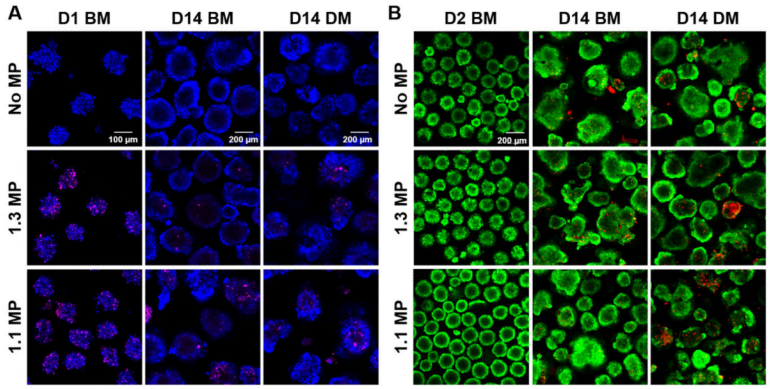


**Fig. 1.**

Mineral particle incorporation and cell viability. (A) Xylenol orange-labeled MPs (pink) were incorporated and persisted within the ESC aggregates for up to 14 days of culture in either basal media (BM) or differentiation media (DM). Calcein AM-stained ESCs were pseudocolored as blue. (B) Live/Dead staining of D2 and D14 ESC aggregates in either BM or DM culture. Live cells were stained by calcein AM (green) while dead cells were stained by ethidium homodimer-1 (red).

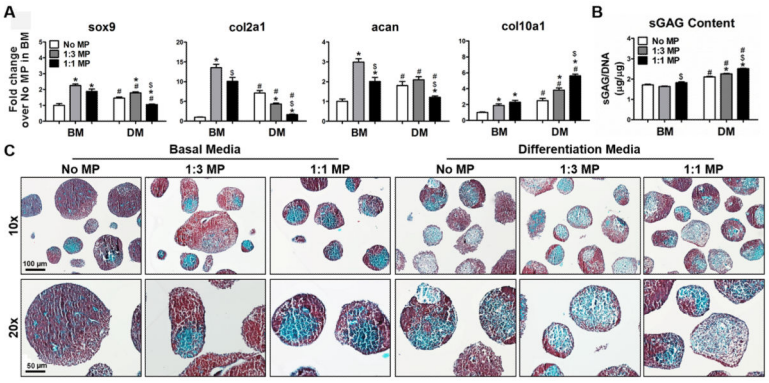


**Fig. 2.**

Chondrogenesis of ESC aggregates with incorporated MPs. ESC aggregates were cultured for 14 days in either basal media (BM) or differentiation media (DM). (A) Real-time PCR analysis of gene expression of chondrogenic markers. (B) SGAG content extracted from ESC aggregates was quantified by DMMB assay and normalized to DNA content. n=4, *P<0.05 *vs.* No MP, $P<0.05 *vs.* 1:3 MP under the same culture condition, #P<0.05 *vs.* BM. (C) sGAG deposition (red) in aggregates was visualized by safranin O and fast green counterstaining.

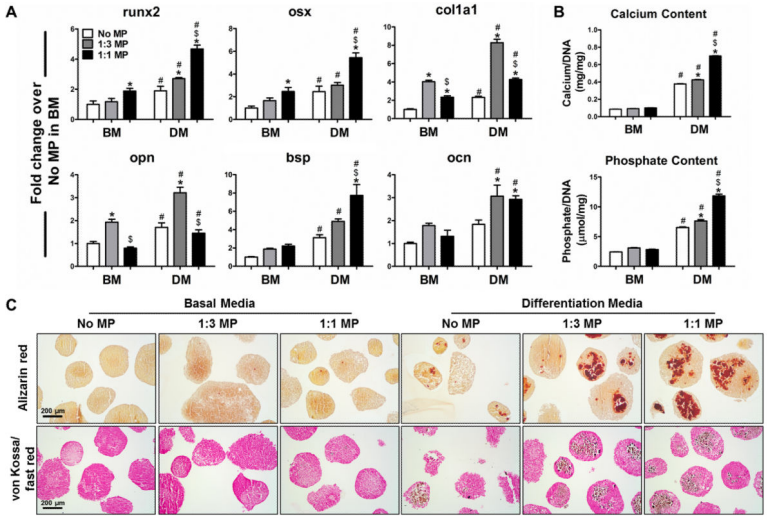


**Fig. 3.**

Osteogenesis of ESC aggregates with incorporated MPs. ESC aggregates were cultured for 14 days in either basal media (BM) or differentiation media (DM). (A) Real-time PCR analysis of the gene expression of osteogenic markers. (B) Phosphate and calcium content extracted from aggregates were quantified colorimetrically and normalized to DNA content. n=4, *P<0.05 *vs.* No MP and $P<0.05 *vs.* 1:3 under the same culture; #P<0.05 *vs.* BM. (C) The presence of calcium and phosphate deposition within ESC aggregates was visualized by alizarin red staining (red) and von Kossa (black) / fast red counter staining, respectively.

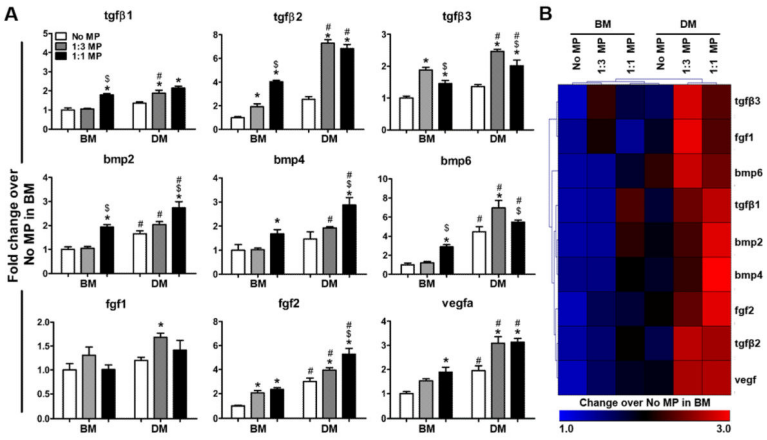


**Fig. 4.**

Effect of mineral particles on growth factor expression. (A) Real-time PCR analysis of gene expression of various growth factors by ESC aggregates after 14 days of culture in either basal media (BM) or differentiation media (DM). n=4, *P<0.05 *vs.* No MP under the same culture; $P<0.05 *vs.* 1:3 MP under the same culture; and #P<0.05 *vs.* BM. (B) Hierarchical clustering of heat map representation of results illustrates the differences in the gene expression of growth factors among different groups.

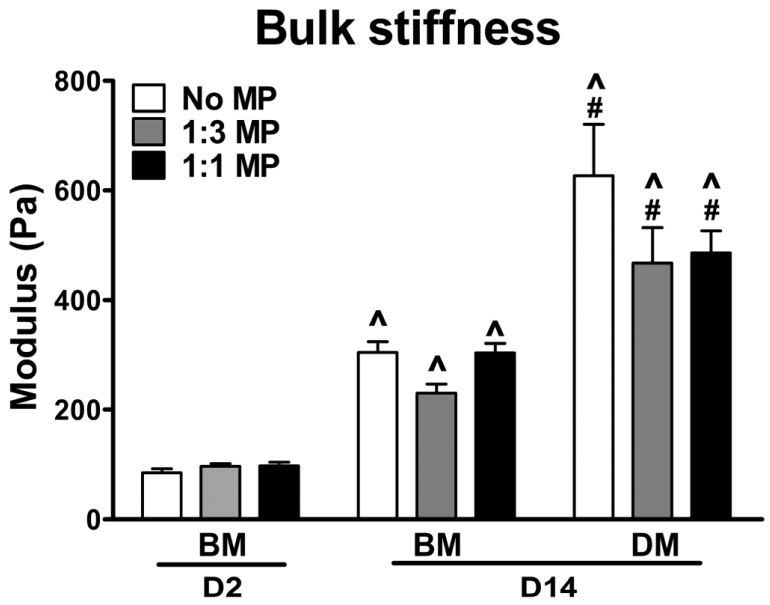


**Fig. 5.**

Effect of mineral particles on bulk stiffness of ESC aggregates. The bulk stiffness of ESC aggregates after 2 days or 14 days of cultures were measured via parallel plate compression testing. n=8 for each group, ^P<0.05 vs. D2 BM, $^{\#}$P<0.05 *vs.* D14 BM.

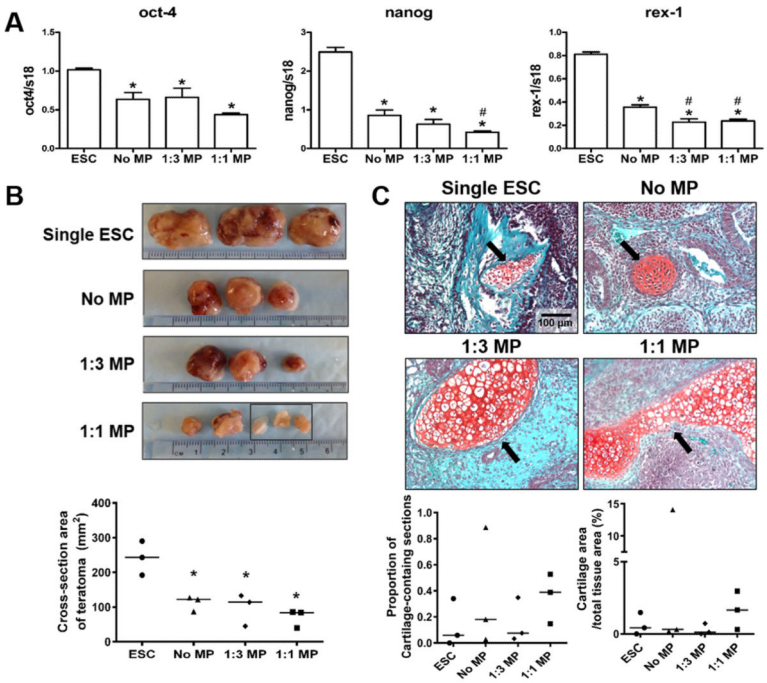


**Fig. 6.**

Effect of mineral particles on the pluripotency of ESC aggregates. (A) Real-time PCR analysis of pluripotent gene expression. *P<0.05 vs. single ESCs (n=4). (B) Equal cell numbers of single ESCs (ESC suspension harvested directly from 2D culture), no MP, 1:3 MP, or 1:1 MP ESC aggregates were subcutaneously injected in NOD SCID mice and the tissue masses were harvested 28-days post-injection and examined macroscopically. Black rectangle indicates the three individual pieces of teratoma derived from a single injection of 1:1 MP aggregates. The cross-section area of teratomas were quantified by Image J. *P<0.05 vs. single ESCs. (C) Teratoma sections were stained by safranin O/fast green in order to visualize the positive-stained cartilage tissues (red) within each section. Representative images of stained teratomas sections showed the presence of cartilage tissues as indicated by arrows (Scale bar = 100 μm). The proportion of cartilage-containing sections and the cartilage cross-sectional area % were calculated based on histomorphometric analyses.

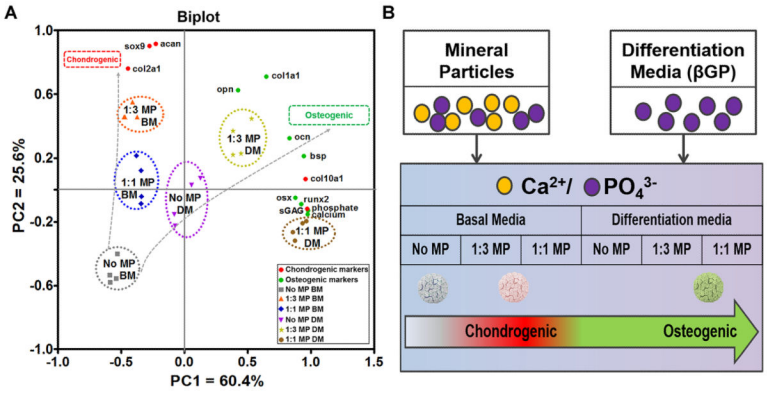


**Figure 0007**

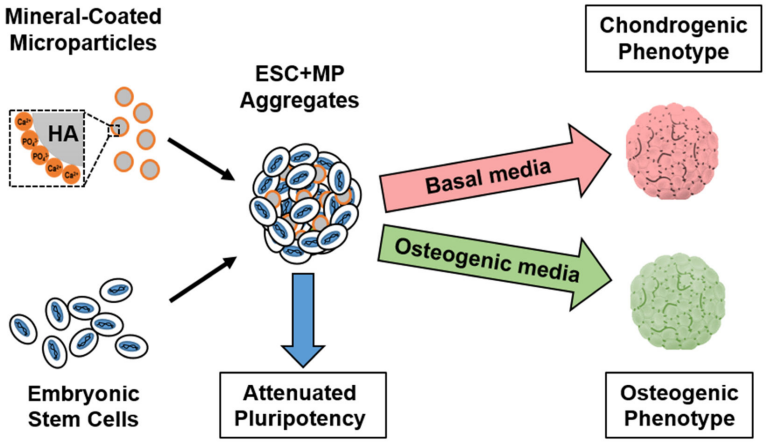


**Figure 0008**

**Fig. 7.**

Summary of the effects of MPs on the osteochondral differentiation of ESCs. (A) PCA biplot illustrated the effect of MP incorporation in combination with different culture conditions on ESC osteo-chondrogenic phenotypes. The dotted ellipses represent clustering of individual treatment groups. (B) Schematic model of MP-induced osteo-chondrogenic differentiation of ESC aggregates.